

## Diffusion in a two-dimensional energy landscape in the presence of dynamical correlations and validity of random walk model

Subhajit Acharya  and Biman Bagchi \**Solid State and Structural Chemistry Unit, Indian Institute of Science, Bengaluru 560012, India*

(Received 15 September 2022; revised 30 December 2022; accepted 26 January 2023; published 16 February 2023)

Diffusion in a multidimensional energy surface with minima and barriers is a problem of importance in statistical mechanics and it also has wide applications, such as protein folding. To understand it in such a system, we carry out theory and simulations of a tagged particle moving on a two-dimensional periodic potential energy surface, both in the presence and absence of noise. Langevin dynamics simulations at multiple temperatures are carried out to obtain the diffusion coefficient of a solute particle. Friction is varied from zero to large values. Diffusive motion emerges in the limit of a long time, even in the absence of noise. Noise destroys the correlations and increases diffusion at small friction. Diffusion thus exhibits a nonmonotonic friction dependence at the intermediate value of the damping, ultimately converging to our theoretically predicted value. The latter is obtained using the well-established relationship between diffusion and random walk. An excellent agreement is obtained between theory and simulations in the high-friction limit but not so in the intermediate regime. We explain the deviation in the low- to intermediate-friction regime using the modified random walk theory. The rate of escape from one cell to another is obtained from the multidimensional rate theory of Langer. We find that enhanced dimensionality plays an important role. To quantify the effects of noise on the potential-imposed coherence on the trajectories, we calculate the Lyapunov exponent. At small friction values, the Lyapunov exponent mimics the friction dependence of the rate.

DOI: [10.1103/PhysRevE.107.024127](https://doi.org/10.1103/PhysRevE.107.024127)

### I. INTRODUCTION

The relationship between diffusion and friction was first derived by Einstein in his classic work on Brownian motion [1] in 1905, where the single-particle transport rate diffusion ( $D$ ) was related to friction ( $\zeta$ ) on the particle by  $D = k_B T / \zeta$ . This simple relation may define friction, particularly in liquids, aided further by the Langevin equation. In many studies, the above relation or its generalization is used to obtain friction, for example to obtain the effects of friction and viscosity on the rate of a chemical reaction [2,3].

We note that friction is a linear-response function, and Einstein's relation is a statement of linear-response theory [2]. These are expected to be valid across systems, although the nature of friction can be complex in systems such as diffusion on an energy landscape with maxima and minima. The motion of a particle in a potential energy landscape finds applications in many branches of physics, chemistry, and biology to discuss diverse problems [4–6]. In these examples, diffusion usually involves crossing barriers in the presence of noise [7,8].

In some cases, diffusion in a complex energy landscape can be modeled as a random walk where the transition rate between the sites (or cells, basins) depends on friction or viscosity. Here diffusion is given by  $D = (1/2d)ka^2$ , where  $D$  is the value of the diffusion coefficient,  $d$  is the dimension of the

system,  $a$  is the distance between two adjacent minima, and  $k$  is the rate of transition between two adjacent sites. When the rate is inversely proportional to friction, the diffusion inherits the same frictional dependence as given by Einstein through a simple random walk model [9,10]. There would appear, however, to be a nontrivial temperature dependence determined by certain characteristic features of the barrier that the random walker needs to surmount. Another example is provided by Zwanzig's solution of diffusion in a rugged energy landscape, discussed further below [11,12]. These models lead to the following form of the relation between diffusion and friction:

$$D = \frac{k_B T}{\zeta} F(T), \quad (1)$$

where the temperature-dependent factor  $F(T)$  contains such effects of the potential energy surface as the barrier height, barrier frequency, etc. Equation (1) can be regarded as a generalization of the celebrated Einstein's relation between diffusion and friction discussed above.

As pointed out above, Eq. (1) can be useful in wide-ranging problems where diffusion occurs in the presence of a potential energy landscape. However, most general studies employed only a one-dimensional potential energy description because the established technique of mean first passage time with an absorbing/reflecting barrier is usually not available in higher dimensions. There are interesting issues that have drawn attention. We note that Newman and Stein earlier had established that diffusion in a one-dimensional rugged energy landscape could be "pathological" [13]. The same is removed in higher dimensions. Banerjee *et al.* have

\*Corresponding author: [bbagchi@iisc.ac.in](mailto:bbagchi@iisc.ac.in);  
[profbiman@gmail.com](mailto:profbiman@gmail.com)

confirmed these predictions by employing computer simulations [14]. A theoretical study that generalizes Zwanzig's original mean first passage time calculation was presented by Seki and Bagchi [15], and the new expression for the effective diffusion coefficient  $D(\delta, \sigma)$  is given by

$$D(\delta, \sigma) = D_0 \exp\left(-\frac{\delta^2}{(k_B T)^2}\right) / \left[1 + \operatorname{erf}\left(\frac{\delta}{2k_B T} \sqrt{1 - \exp(-a^2/2\sigma^2)}\right)\right]. \quad (2)$$

In this formalism, one-dimensional potential energy  $U(x)$  is composed of a background smooth potential  $U_0(x)$  and a rugged potential  $U_1(x)$ , i.e.,  $U(x) = U_0(x) + U_1(x)$ . Here  $D_0$  is the bare diffusion coefficient in the absence of a rugged landscape. This model assumes that site energies on the lattice positions have Gaussian correlations, i.e.,  $\langle U(0)U(x) \rangle = \delta^2 \exp(-a^2 x^2/2\sigma^2)$ . Here  $\sigma$  is the correlation length,  $a$  denotes the lattice spacing,  $k_B$  is the Boltzmann constant,  $T$  denotes temperature, and  $\delta$  measures the root mean squared roughness of the potential energy surface. This expression was found to be quantitatively reliable. Note that the form given by Eq. (1) is preserved but valid only in the overdamped limit (high-friction limit).

A systematic study of the combined effects of noise and potential energy surface on diffusion is relatively rare for higher dimensions. Festa and d'Agliano studied diffusion for a Brownian particle in a periodic field of force in the overdamped limit [16]. In that particular case, they obtained an eigenvalue solution for the long-time diffusion coefficient, which is given by

$$D = \frac{a^2}{2d} [\nabla_{k\alpha} \nabla_{k\alpha} \lambda(k, 1)]_{k=0}, \quad (3)$$

with the eigenvalue taking the form  $\lambda(k, \alpha) = \frac{k_B T}{\zeta} \Lambda(k, \alpha)$ . Here  $\Lambda$  represents the dimensionless non-negative parameter and depends on the characteristic nature of the potential energy surface. In Eq. (3),  $d$  denotes the dimension,  $\alpha$  is a band index familiar in the quantum theory of solids,  $k$  denotes a generic vector of the reciprocal space ranging in the first Brillouin zone, and  $a$  is the interplanar spacing of a crystal [16]. This exciting study bears a resemblance to Langer's well-known analysis of rate across a barrier in a multidimensional potential energy surface [17]. In Langer's analysis, the rate is also given by an eigenvalue that defines the unstable mode and applies to the overdamped limit.

In recent years, there have been impressive developments in the numerical evaluation of the multidimensional free-energy surface [18–22]. Many of these studies were motivated by the pioneering analytical studies of Onuchic and Wolynes, who modeled protein folding as a configuration space diffusion on a rugged two-dimensional free-energy surface where the collective variables were the size of the protein and the contact order parameter [4,8]. Most of the recent numerical calculations, such as protein folding and protein association-dissociation reactions, have used metadynamics, umbrella sampling, and more sophisticated techniques, and they concentrated mainly on two-dimensional free-energy surfaces [23,24]. A substantial amount of discussion has focused on the criteria for selecting the appropriate order parameters [25,26].

In our earlier work, we discussed those aspects in the context of insulin dimer dissociation [27,28]. We observed that the choice of appropriate order parameters might depend on the stage of the complex reaction. While at significant separation, the center-to-center distance is the desired order parameter. More specific quantities, such as contact between two helices, each from one monomer, provide a better description at close separation.

While substantial effort has been devoted to calculating the multidimensional free-energy surface, less effort has been directed toward the calculation of the rate or diffusion. Recent rate theory developments suggest that frictional effects arising from a solvent can influence the reaction rate considerably along with barrier height [29,30]. As we have experienced in the study of one-dimensional activated barrier crossing dynamics, where the frictional effects can reduce the rate by more than one order of magnitude, similar effects can be operative in multidimensional barrier crossing dynamics [29].

In the present work, we study the diffusional dynamics of a Brownian particle in a periodic and continuous-potential analog of regular Lorentz gas where the potential energy surface in two dimensions is given by [32]

$$V(X, Y) = \varepsilon \left[ \cos(X + Y/\sqrt{3}) + \cos(X - Y/\sqrt{3}) + \cos(2Y/\sqrt{3}) \right]. \quad (4)$$

Here  $\varepsilon$  is the energy scaling constant described later. The potential function is depicted in Fig. 1. It is evident that a study of diffusion in this periodic cosine potential can also be relevant to various applications such as superionic conductors, the motion of adsorbates on crystal surfaces, polymers diffusing at the interfaces, molecular graphene, etc. [31–33]. Moreover, as we demonstrate, even such an apparently simple system can exhibit rich dynamical features.

In this work, we ask the following questions:

(i) What is the nature of diffusion in the zero- and very low-friction limit when the migration of a tagged particle depends on the details of the potential energy surface? How do we characterize the emergence of diffusion? For diffusion to emerge, the dynamical system must become chaotic.

(ii) Is it possible to discuss chaos quantitatively for this system? Does the divergence rate between two trajectories in the phase space exhibit a similar dependence on frictionlike diffusion?

(iii) If diffusion is found to exist, can we describe it as a random walk model? It is commonly believed that diffusion should have an underlying random walk picture.

(iv) How do we analytically calculate the diffusion coefficient values as we vary noise and temperature?

(v) How do we estimate the escape rate of the Brownian particle from the minimum of the initial cell by employing multidimensional rate theories and connect it with diffusion?

(vi) Is it possible to derive a scaling relation between diffusion and entropy starting from the basic principles of statistical mechanics for this system?

We obtain the answers to the above questions using a mix of analytical and numerical techniques.

The rest of the article is organized as follows. In Sec. II, we detail the studied system and simulation methodology. Section III A presents the nonmonotonic behavior of the noise-driven

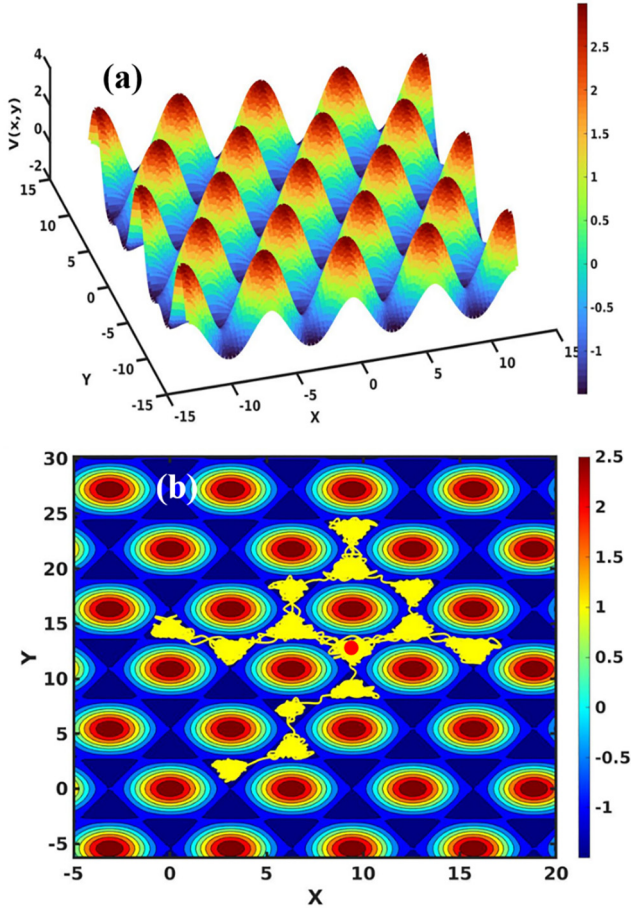


FIG. 1. (a) A schematic representation of the two-dimensional potential energy function defined in Eq. (4). The range and color codes are given on the right side of the plot. (b) The time evolution of a long trajectory is shown on the two-dimensional representation of the potential energy function. Here the yellow line represents the trajectory of a Brownian particle starting at the minimum of a cell. The red circle represents the initial configuration of the particle in the phase space. Note that the trajectory makes multiple returns to the initial cell, indicating the presence of correlations, discussed further in the text. Here  $X$  and  $Y$  are in the reduced units.

diffusion against friction. Section III B measures the chaos by computing the Lyapunov exponent. Section III C calculates the barrier crossing rate using different theoretical and numerical schemes. In Sec. III D, we validate the random walk model in the presence of crossing and recrossing. We adopt a modified random walk formalism to address the long-range correlated returns, specifically in the low-friction regime in Sec. III E. A discussion on the exponential scaling relation between diffusion and entropy for a particle following Langevin dynamics is presented in Sec. III F. Finally, Sec. IV summarizes our work and draws some general conclusions.

## II. SYSTEMS AND SIMULATIONS

In our system, the Brownian particle moves on a two-dimensional periodic potential given by Eq. (4), and the equation of motion is governed by the ordinary Langevin

equation [Eq. (5)],

$$\frac{dv}{dt} = -\zeta v + \frac{1}{m}F(X, Y) + R(t), \quad (5)$$

with  $\langle R(t) \rangle = 0$ ,  $\langle R(t)R(t') \rangle = 2\zeta k_B T \delta(t-t')$ .

Here  $v$  denotes the velocity of the particle at time  $t$ ,  $F(X, Y)$  is the two-dimensional force experienced by the tagged particle,  $m$  is the mass of the particle,  $\zeta$  denotes friction coefficient, and the noise  $R(t)$  denotes the random or fluctuating force. The fluctuating force arises from occasional impacts of the Brownian particle with molecules of the surrounding medium. Therefore, the noise  $R(t)$  is a centered Gaussian white noise with the covariance of  $2\zeta k_B T \delta(t-t')$ . The fluctuation-dissipation theorem relates the strength of random noise ( $B$ ) with the coefficient of friction ( $\zeta$ ) via the relation  $B = \zeta k_B T$ . Temperature enters the calculation through the fluctuation-dissipation theorem described above [34,35].

We project the potential energy function defined in Eq. (4) in the two-dimensional  $X$ - $Y$  plane, and we find that each cell contains a minimum at the center of the triangle, maxima at the three corners of the triangle, and saddle points at the midpoints of the edges, as shown in Fig. 1(b). Energies of the maxima, minimum, and saddle points of each cell are given by  $3.0\varepsilon$ ,  $-1.5\varepsilon$ , and  $-1.0\varepsilon$ , respectively. Initially, a Brownian particle is placed near the minimum of the triangular cell to have an energy-minimized configuration, as shown by the red circle in Fig. 1(b). The velocity of the particle is assigned according to the equilibrium Maxwell distribution at a fixed temperature. We carry out all the analyses for 2000 different initial configurations. We use Gear's fifth-order predictor-corrector algorithm to integrate the equation of motion of the particle because of its stability throughout the entire friction range with time step  $0.001\tau$  [36,37], where  $\tau = \sqrt{(m\sigma^2/\varepsilon)}$  is the unit of time with  $m$  the mass,  $\sigma$  is the unit of length, and  $\varepsilon$  is the unit of energy. In our study, we follow the conventional way of dealing with the reduced quantities in molecular-dynamics simulation, and we stick to that throughout the work. We perform all the calculations for 2000 different initial configurations to obtain a statistically significant and reproducible result at two reduced temperatures,  $T^* = 0.1$  and  $0.2$ , with  $\sigma = 1$ ,  $\varepsilon = 1$ , and  $m = 1$ . We basically study a point particle here. A virtual size or mass is provided in order to make a connection to the real units.

## III. RESULTS AND DISCUSSIONS

### A. Nonmonotonic behavior of noise-driven diffusion

The diffusional dynamics of a particle in this system are complex due to a refocusing of trajectories caused by a concave curvature in the potential energy surface, as shown in Fig. 1(b). This is to be regarded as the opposite to dispersion caused by a convex surface. This concavity causes an additional, long time (as opposed to short time, collisional) trapping of the trajectories, causing back-and-forth journeys between the same two cells. In an isolated system where the existence of diffusion is solely the consequence of interactions

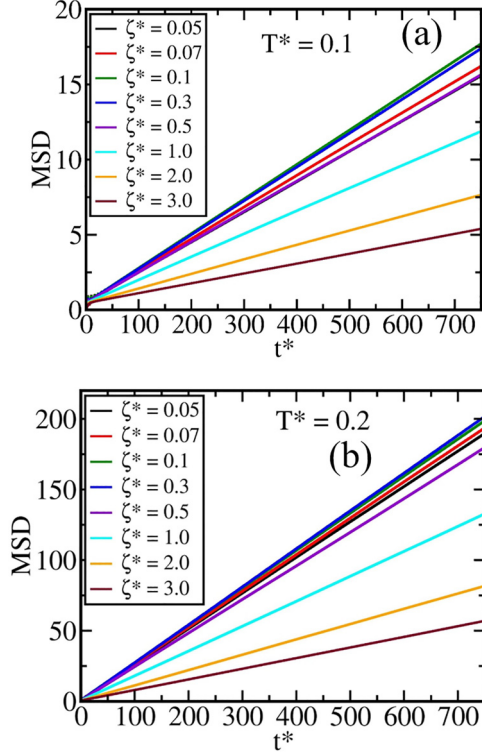


FIG. 2. The plot of MSD against time for different values of friction at reduced temperatures: (a)  $T^* = 0.1$  and (b)  $T^* = 0.2$ . After a short ballistic motion, MSD grows linearly with time in both cases. The slope of the plot in the linear regime provides a measure of the self-diffusion coefficient, which displays a nonmonotonic behavior against friction.

with the potential energy surface, such refocusing lowers diffusion significantly.

### 1. Diffusion in the presence of friction

This subsection demonstrates the diffusion behavior in the presence of friction at two reduced temperatures,  $T^* = 0.1$  and  $0.2$ . We calculate the self-diffusion coefficient ( $D$ ) of the Brownian particle using Einstein's relation between  $D$  and the mean-square displacement (MSD). In two dimensions, the self-diffusion coefficient is defined by

$$D = \lim_{t \rightarrow \infty} \frac{\langle (\mathbf{r}(t) - \mathbf{r}(0))^2 \rangle}{4t}, \quad (6)$$

where  $\mathbf{r}(t)$  is the position of the particle at time  $t$ , and angular brackets indicate the ensemble average. In Fig. 2, we plot MSD against time for different values of friction at two reduced temperatures,  $T^* = 0.1$  and  $0.2$ . In both figures, we observe that MSD grows linearly with time after the correlation time, and its slope in the linear regime provides the self-diffusion coefficient [Eq. (6)].

In our study, both the inertia effect and the characteristic nature of the potential energy surface play a vital role in inducing correlation in the system. We plot the well-converged diffusion values against friction (i.e., in the range  $\zeta^* \geq 0.05$ , where the noise strength is sufficient to make the motion diffusive) in Fig. 3 at two reduced temperatures. The results

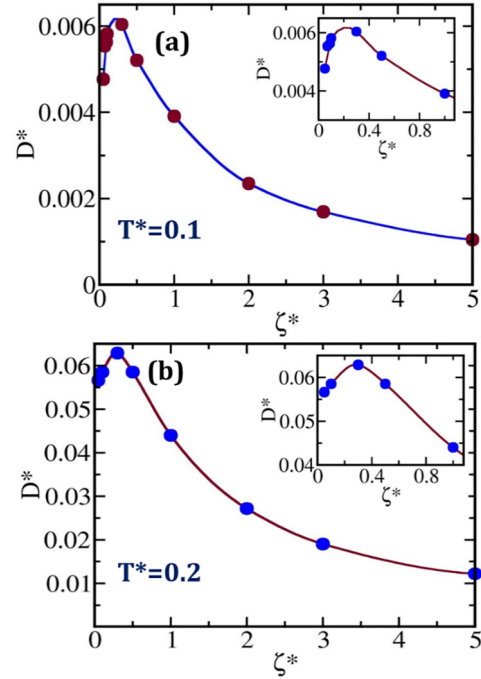


FIG. 3. Variation of self-diffusion coefficients against friction (in the range 0.05–5.0) at two reduced temperatures (a)  $T^* = 0.1$  and (b)  $T^* = 0.2$ . We estimate the self-diffusion coefficient of the Brownian particle by employing Eq. (6), and we plot it against friction here. Diffusion exhibits a nonmonotonic dependence on friction in both cases. The inset shows the variation of  $D^*$  as a function of friction, specifically in the low-friction region. The line joining the data points is provided as a guide to the eyes.

are expressed in dimensionless units where [38]

$$E^* = \frac{E}{\varepsilon}, \quad T^* = \frac{k_B T}{\varepsilon}, \quad X^* = \frac{X}{\sigma}, \quad Y^* = \frac{Y}{\sigma},$$

$$\tau = \sqrt{\frac{m\sigma^2}{\varepsilon}}, \quad t^* = \frac{t}{\tau}, \quad D^* = \frac{D\tau}{\sigma^2}, \quad \text{and} \quad \zeta^* = \zeta\tau.$$

Here  $D^*$  denotes the reduced self-diffusion coefficient,  $\zeta^*$  denotes the reduced friction,  $E^*$  is the reduced total energy,  $T^*$  is the reduced temperature, and  $t^*$  indicates the reduced time.

Figure 3 shows an interesting nonmonotonic friction dependence of the diffusion at two different temperatures. A similar kind of nonmonotonic behavior of diffusion is observed in an earlier study where a tagged particle moves among fixed spherical crowders [39]. In this system, the tagged particles interact with the crowders through a combination of hard-core repulsion and short-range attraction. Effective diffusion is found to exhibit a nonmonotonic behavior against the strength of the attractive potential between crowders and tagged particles. In the presence of a large attraction, it is perhaps not too difficult to understand that diffusion decreases with the increase in the strength of attraction. The accelerated diffusion in the presence of small attraction is reminiscent of the phenomenon of facilitated diffusion. It should be noted that in the above-mentioned work, all the calculations are performed in the overdamped limit only. However, in our work we investigate the diffusive

dynamics of the Brownian particle from the low-friction limit to the high-friction limit. This nonmonotonic dependence of diffusion on friction has two nontrivial origins.

(i) Because of recrossing induced by the concave nature of the potential energy surface superimposed on the maximum, diffusion is low in the very low-friction regime. There is a proportional relation between friction and noise following the fluctuation-dissipation theorem [2]. The initial increase in diffusion with friction happens because the particle enters the energy-controlled region where the sole energy source comes from colliding with the surrounding solvent. Noise destroys the coherence and serves to increase diffusion as we move from low- to intermediate-friction regions. However, in the overdamped limit, localization of the trajectories happens in configurational space, which lowers diffusion (discussed later). This is why we would not be observed the nonmonotonic behavior in the overdamped limit. This is somewhat novel and could be present in some cases.

(ii) A second reason (discussed more later) is the non-monotonic friction dependence of the barrier crossing rate. This is a two-dimensional version of Kramers' turnover, well-known in chemical kinetics [30,40]. These two are intimately connected.

We can obtain the self-diffusion coefficient also by integrating the unnormalized velocity autocorrelation. According to the Green-Kubo formalism,  $D$  is defined as

$$D = \frac{1}{d} \int_0^\infty \langle \mathbf{v}(t) \cdot \mathbf{v}(0) \rangle dt, \quad (7)$$

where  $d$  indicates the dimension of the system, and  $\mathbf{v}(t)$  is the velocity vector of the particle at time  $t$ . We define the normalized velocity autocorrelation function as  $C_v(t) = \langle \mathbf{v}(0) \cdot \mathbf{v}(t) \rangle / \langle \mathbf{v}(0)^2 \rangle$ , and we plot it against time at two reduced temperatures for different friction values in Fig. 4. We observe that  $C_v(t)$  for the system without friction shows a pronounced long-time oscillatory behavior, which gradually decreases with the increasing strength of friction. The oscillatory behavior of the velocity autocorrelation function is a consequence of the combined effect of inertia and potential energy landscape. However, it is vastly dominated by the characteristic nature of the potential energy landscape. This exciting observation brings about the following subsection to explore the diffusional dynamics of a particle in the absence of friction in more detail, where the inertia effect plays no role. We perform the Fourier transformation of the velocity autocorrelation function, and we find that the peak height at a comparably higher frequency gradually decreases with the increase in friction at two temperatures (see the Supplemental Material [65] for details, SM-S1).

### 2. Study of diffusion in the absence of friction

In the study of diffusion phenomena, diffusion is inevitably correlated with friction through Einstein's relation and the Langevin equation. However, one can observe diffusion even in the absence of friction or noise exerted externally. The appearance of diffusion in a deterministic system (i.e., in the absence of noise) is intimately connected with the existence of ergodicity and chaos. The emergence of ergodicity in a deterministic system was studied by Bunimovich and Sinai

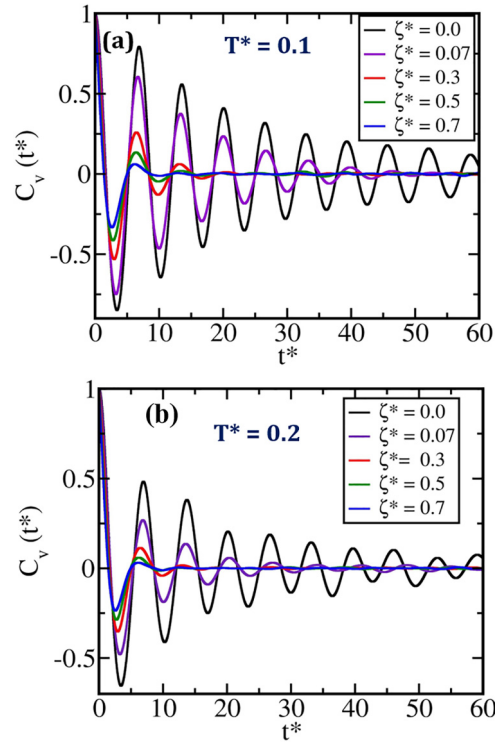


FIG. 4. (a) The plot of the normalized velocity autocorrelation function  $C_v(t^*)$  against time at a reduced temperature  $T^* = 0.1$ . Here, we show the variation of  $C_v(t^*)$  for several friction values (like  $\zeta^* = 0.0$ ,  $\zeta^* = 0.07$ ,  $\zeta^* = 0.3$ ,  $\zeta^* = 0.5$ , and  $\zeta^* = 0.7$ ). (b) The same is plotted at a reduced temperature  $T^* = 0.2$ . In (a) and (b), we observe the oscillatory nature of  $C_v(t^*)$ , which is prominent in the absence of friction, and gradually diminishes with the increasing strength of friction.

in a two-dimensional system of hard disks [41]. Machta and Zwanzig studied similar issues in a regular Lorentz gas [42].

In the absence of friction, the system becomes isolated from the surroundings, and Newton's equation governs the equation of motion of the particle. In this limit, the particle gets trapped near the minimum of the initial triangular cell forever, as is evident in Fig. 7(a), when its total energy is below the saddle point energy, i.e.,  $E_S = -1.0\epsilon$ . However, the system with energy just above the saddle energy exhibits a coherence where the trajectory gets refocused after reaching the end of the adjacent cell and turns back to shuttle between the two cells [as shown in Fig. 7(b)]. As a result, the motion becomes chaotic, and diffusion exists in this system. Towards this goal, we investigate the variation of the normalized velocity autocorrelation function against time with increasing strength of the total energy in Fig. 5.

It is important to note that we perform an average over only the initial Maxwell distribution in this limit. In Fig. 5, we observe that as we increase the total energy of the particle, the oscillatory nature of the velocity autocorrelation function decreases. Increasing the strength of the total energy lowers the probability of getting trapped near the minimum of a cell. This observation can be quantitatively rationalized by performing a Fourier transformation of the velocity autocorrelation function, as demonstrated in our earlier studies [32,43].

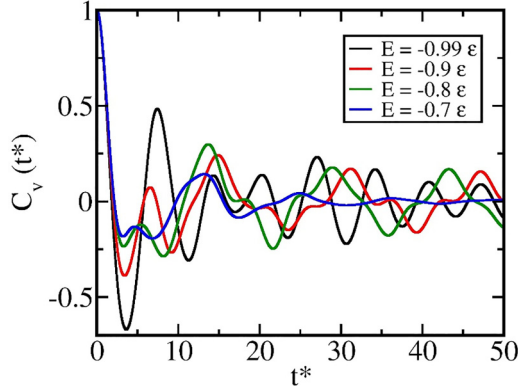


FIG. 5. The plot of the normalized velocity autocorrelation function  $C_v(t^*)$  against time in a deterministic isolated system. We observe that with the increasing total energy of the system, the velocity correlation function starts converging at a faster rate. The oscillations are mainly due to trapping near the minimum of a triangular cell. The oscillatory nature of the velocity correlation functions gradually decreases with energy since the probability of getting trapped decreases with the increasing strength of the total energy.

Since we observe oscillations in the isolated system where inertia plays no role, we can conclude that the characteristic nature of the potential energy plays a dominating role in inducing oscillations over inertia effects in the presence of friction. The existence of diffusion in the absence of friction requires the total energy of the particle to be higher than the saddle energy. To extract a well-converged diffusion in this regime, one needs to carry out a long simulation.

### B. Onset of chaotic motion and crossover behavior in a Lyapunov exponent

In the absence of friction, the system studied is fully deterministic. In this limit, the trajectories are getting strongly mixed within each trapping region in the configurational phase space because of the characteristic nature of the potential energy surface. This can happen in a deterministic system when collisions between the particle and the scatterer become dispersive. As a result, the motion of the particle becomes chaotic. On the other hand, noisy and chaotic motions are two distinct phenomena. In a noisy system, sensitivity to initial conditions is due to a mechanism fundamentally different from deterministic chaos. Therefore, a positive Lyapunov exponent cannot be considered a hallmark of chaos in a stochastic system. We indeed require sophisticated mathematical tools to discriminate the two phenomena [44,45]. However, the present study does not investigate these two in great detail since it aims to study the role of noise on the diffusional dynamics and kinetics of the tagged particle moving on the two-dimensional periodic potential energy landscape.

To measure the average exponential rate of divergence or convergence of near orbits in the phase space, it is convenient to compute the Lyapunov exponent ( $L_n$ ) [46–48]. We study the Lyapunov exponent to understand the character of the motion. In this context, we employ a “shadow trajectory” formalism

to estimate  $L_n$ , as given by [48]

$$L_n = \frac{1}{n\Delta t} \sum_{i=1}^n \ln \frac{d_i}{d_{i-1}}. \quad (8)$$

To implement this formalism, we initially choose two arbitrary close points separated by a distance ( $d_0$ ), and we monitor their mutual separation ( $d_i$ ) with time. Here  $d_i$  is the distance between two trajectories at the  $i$ th time step, and  $d_{i-1}$  is the same at the  $(i-1)$ th time step. In Eq. (8), ( $n$ ) counts the step number, and  $\Delta t$  is the time interval between two steps. It should be noted that, during the process, we need to renormalize the distance between the two selected trajectories periodically. We detail the numerical procedure employed to renormalize the distance between two close trajectories in Sec. SM-S3 of the Supplemental Material (SM) [65]. After each 10-time-step interval, we rescale the separation vector to its initial length. This procedure generates a time average over the two trajectories that start at close proximity in the phase space. If we plot  $L_n$  against  $n$ , it saturates after initial oscillations, allowing  $L_n$  to be estimated unambiguously, as shown in Fig. S4 of the SM [65].

Figure 6 plots  $L_n$  against friction at two reduced temperatures (i.e.,  $T^* = 0.1$  and  $0.2$ ). The calculated Lyapunov exponent exhibits an interesting dependence on friction. In Fig. 6, we observe two significant trends. In the energy-controlled regime (i.e., at low friction),  $L_n$  rises sharply with friction. However, in the intermediate- to high-friction region, the calculated  $L_n$  exhibits a slow decay with the increase in friction. In the inset, we show the variation of  $L_n$  with friction, emphasizing the overdamped limit. The inset shows that the divergence rate between two trajectories decreases with the increase in friction in the high-friction limit.

In the energy-controlled regime, the motion of the Brownian particle is primarily dictated via collisions with the surrounding solvent molecules. Therefore, the divergence rate of the two close trajectories increases with the slight increase in friction in this regime. However, beyond a particular value of friction, the system enters the diffusion-controlled regime where frictional effects slow down the motion of the particle. As discussed later, the analogy is similar to Kramer’s turnover problem. In this regime, the frictional effects favor the localization of the trajectory in the phase space, which tends to reduce the Lyapunov exponent slightly. We estimate the Lyapunov exponent of the isolated system in order to capture the role of the potential energy surface when the total energy of the particle ( $E = -0.99\epsilon$ ) exceeds the saddle point energy (i.e.,  $E_S = -1.0\epsilon$ ), as shown by the black dotted line in Fig. 6. We find that the Lyapunov exponent of the system following Langevin dynamics is higher than that of the isolated system. This is expected, and we take this as a signature of correct dynamical behavior. In the presence of friction, the combined effect of the potential energy surface and noise plays an essential role in increasing the divergence rate of the two trajectories.

To make the discussion more concrete, we carry out trajectory analysis in Fig. 7 for some specific friction values. In the absence of friction and with an energy content below the saddle point energy, the particle remains trapped near the minimum of the initial cell, as shown in Fig. 7(a). However, the

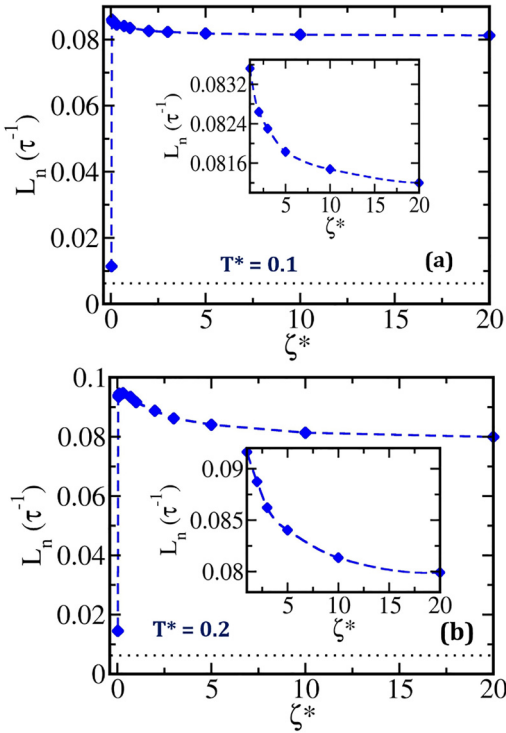


FIG. 6. Plot of the calculated Lyapunov exponent ( $L_n$ ) against friction at two reduced temperatures (a)  $T^* = 0.1$  and (b)  $T^* = 0.2$ . Here we employ Eq. (8) to obtain the Lyapunov exponent for different friction values at two reduced temperatures. We observe that in the low damping regime,  $L_n$  increases with friction sharply, whereas in the overdamped regime,  $L_n$  does not seem to increase rapidly due to the slowness of the medium. The inset shows the variation of  $L_n$  against friction, specifically in the high damping regime. In the overdamped limit, frictional effects favor the localization, which reduces the divergence rate of the two close trajectories in the phase space. This is why  $L_n$  decreases with the increase in friction in this limit. The black dotted line measures the Lyapunov exponent for the isolated system when the total energy of the particle ( $E = -0.99\epsilon$ ) exceeds the saddle point energy (i.e.,  $E_S = -1.0\epsilon$ ) in both (a) and (b). This suggests that the motion of the particle is chaotic even in the absence of noise due to the characteristic nature of the potential energy surface. In (a) and (b), the line joining the data points is provided as a guide to the eyes.

particle can explore the configurational space without friction when the total energy is above the saddle energy, as shown in Fig. 7(b). In Fig. 7(c), we plot the trajectory of the Brownian particle at friction  $\zeta^* = 0.3$ . We choose this friction because, at this friction, diffusion becomes maximum, as shown in Fig. 3.

It is evident in Fig. 7(c) that the particle explores the phase space at a faster rate than in the first case within the same time. In contrast, the particle in the overdamped limit (like at  $\zeta^* = 10.0$ ) shows localization in the configurational phase space [as shown in Fig. 7(d)]. The trajectories shown in Fig. 7 are much longer than the natural timescales.

There is one more exciting aspect of the role of noise, as discussed in detail in SM-S5 [65]. As is evident in the time trajectory of the total energy (i.e., Fig. S5 of the SM [65]), the Brownian particle exhibits a nonzero escape rate even when its

TABLE I. We use the exponential function  $a_0 \exp(-\frac{t}{\tau})$  to fit the normalized energy autocorrelation function, i.e.,  $\frac{\langle \delta E(0)\delta E(t) \rangle}{\langle \delta E(0)\delta E(0) \rangle}$  at two reduced temperatures,  $T^* = 0.1$  and  $0.2$ . We report the fitting parameters here in reduced units.

$T^* = 0.1$		$T^* = 0.2$	
$\zeta^*$	$\tau$	$\zeta^*$	$\tau$
0.05	18.57	0.05	15.67
0.07	16.12	0.07	11.49
0.09	14.54	0.09	8.80
0.1	10.88	0.1	8.70

total energy is less than the saddle energy (i.e.,  $E_S = -1.0\epsilon$  in this case). In Fig. 8, we plot the fluctuation of energy relaxation  $\langle \delta E(0)\delta E(t) \rangle$  against time, where  $\delta E(t)$  at time  $t$  is given by  $E(t) - \bar{E}$ .

Here  $\bar{E}$  is the average energy, and  $E(t)$  denotes the total energy of the particle at time  $t$ . From the plot, we observe that the correlation function for the fluctuations of energy relaxes faster with increasing noise strength. We fit the normalized autocorrelation of energy fluctuation given by  $\frac{\langle \delta E(0)\delta E(t) \rangle}{\langle \delta E(0)\delta E(0) \rangle}$  with the exponential function, and we report the fitting parameters in Table I at two reduced temperatures (i.e.,  $T^* = 0.1$  and  $0.2$ ).

According to the fluctuation-dissipation theorem, noise induces dissipation and causes the system to relax back to the equilibrium state. This is why the relaxation time decreases with the increase in friction. This is a classic example of the role of noise. We perform Fourier transformation of energy relaxation and plot it in the frequency plane (i.e., Fig. S6 of the SM [65]) to understand the effects of correlated motions.

### C. Calculation of the escape rate: Comparisons

It is essential to estimate the escape rate of the tagged particle exhibiting the correlated random walk on a periodic potential energy surface. The primary reason for calculating the escape rate is twofold. As we know, in any system, if a diffusion constant exists, one should be able to identify a random walk in a coarse-grain sense. This leads us to probe the regular random walk picture ( $D = 1/4 k a^2$ ), given that we do have, in our model, the lattice point or the cell rather well-defined. Here “ $a$ ” denotes the distance between two adjacent minima, and  $k$  is the escape rate. Therefore, one needs to compute the escape rate from one cell to an adjacent cell to validate the regular random walk model. On the other hand, it is advantageous to have a simple Hamiltonian system like this where all the parameters required for the rate calculation are readily available, and an accurate estimation of the rate constant from the simulation is also feasible. Due to the simplicity of this chosen Hamiltonian system, we can compute the escape rate accurately by invoking both theoretical and simulation formalisms [43]. To calculate the rate of a barrier crossing process, we require several parameters such as well frequencies, barrier height, barrier frequency, friction, etc. [17,37,49]. Let us assume in our isotropic two-dimensional system that  $X$  is the reaction coordinate and  $Y$  is the nonreactive coordinate. We take the second derivative of the potential given by Eq. (4) with respect to the reactive and the nonreactive coordinates at

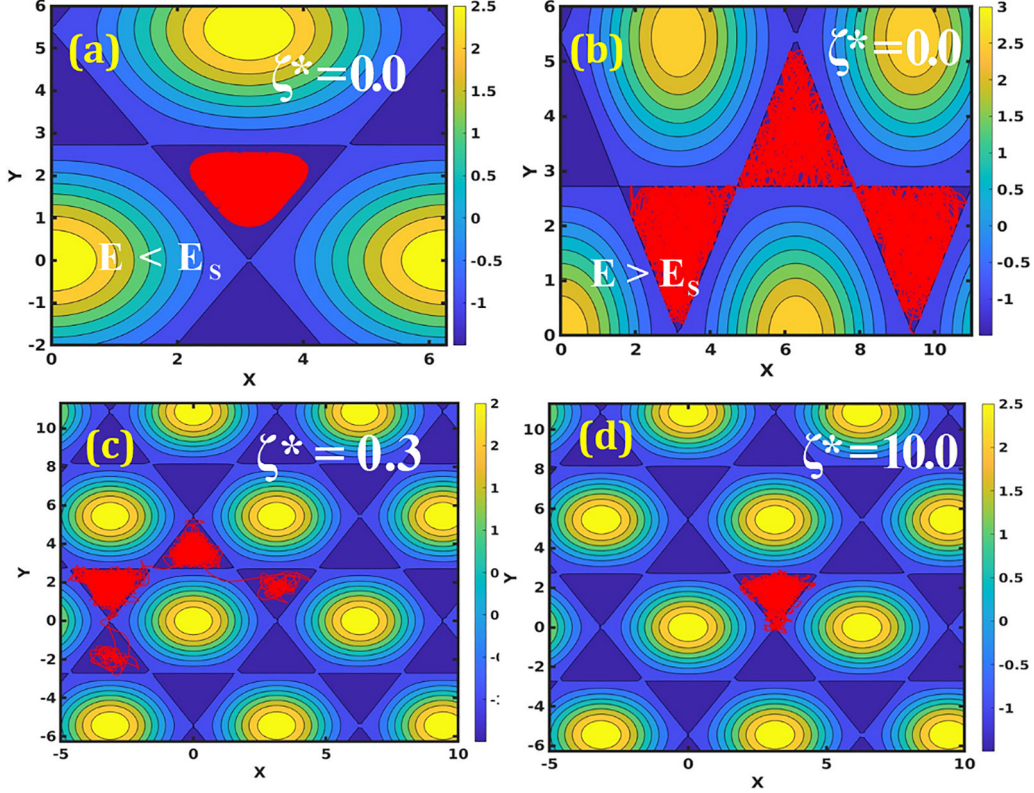


FIG. 7. The time evolution of a long trajectory (i.e.,  $t^* = 5000$ ) of the tagged particle on the two-dimensional potential energy surface shown by the red lines at a reduced temperature  $T^* = 0.1$ . Here  $X$  and  $Y$  are in the reduced units (i.e.,  $X^* = X/\sigma$ ,  $Y^* = Y/\sigma$ ; we have omitted the superscript  $*$  to simplify the notation throughout the study). (a) In the absence of friction, the particle with total energy below  $E_S$  gets stuck inside the original cell, indicating that noise is mandatory for the motion of a particle in this case. (b) We show the trajectory of the particle with total energy (here  $E = -0.99 \varepsilon$ ) above the saddle point energy  $E_S$  in the absence of friction. The particle explores the phase space after spending a long time in each trap region. (c) We show the trajectory of the particle at friction  $\zeta^* = 0.3$ . We choose this particular friction because, at this friction, the diffusion becomes maximum, as discussed before. It clearly shows that the particle moves at a faster rate on the potential energy surface. (d) We demonstrate the trajectory of the particle in the comparably high-friction limit (i.e.,  $\zeta^* = 10.0$  in this case). We observe localization in the configurational space.

the minimum of the initial cell and the saddle to extract well frequency, barrier frequency, etc. In Table II, we report all the parameters required for the theoretical estimate of the escape rate in the reduced unit.

Theoretically, one can estimate the multidimensional rate in several ways [29,49–56]. Our primary aim is to calculate the escape rate for the barrier crossing process going from the minimum of the starting cell to the nearby cell through the available saddle located at the midpoint of the edge. Therefore, the product well does not signify the entire region outside the initial cell, and it is just the minimum of the

adjacent triangular cell separated by a saddle ( $E_S = -1.0\varepsilon$ ). Due to the isotropic nature of the periodic system, the double-well approximation is valid, allowing us to employ standard theoretical methods such as multidimensional transition state theory, Kramers-Langer theory, etc. We employ the multidimensional rate theory given by Langer to obtain the escape rate, which reads [17,29]

$$k_L = \frac{\lambda_+}{2\pi} \left[ \frac{\det E^w}{|\det E^b|} \right]^{1/2} \exp\left(-\frac{E^\ddagger}{k_B T}\right), \quad (9)$$

where  $\lambda_+$  is the only positive root of the equation  $\det(\lambda I + E^b D) = 0$ . Here  $D$  denotes the diffusion matrix, and  $E^w$  and  $E^b$  are the symmetric matrices containing the second partial derivatives of the potential energy at the minima of the initial well and the saddle point, respectively. In Eq. (9),  $E^\ddagger$  denotes the activation barrier. We estimate the rate using Eq. (9), and we plot it against friction in Fig. 9, as shown by the green line at two different reduced temperatures,  $T^* = 0.1$  and  $0.2$ . In the limit of zero friction, Eq. (9) reduces to the transition state theory rate [given by Eq. (12)]  $k_{TST}$ , as shown by the black dotted line in Fig. 9. Since the transition state theory (TST) formalism neglects the effects of friction,  $k_{TST}$

TABLE II. We report the parameters required to calculate the rate along the reactive and the nonreactive coordinates. Here, all the parameters are provided in the reduced units.

Well frequency along $X$ , $\omega_X^w$	$1.0 \tau^{-1}$
Well frequency along $Y$ , $\omega_Y^w$	$1.0 \tau^{-1}$
Barrier frequency along $X$ , $\omega_X^b$	$0.82 \tau^{-1}$
Barrier frequency along $Y$ , $\omega_Y^b$	$1.41 \tau^{-1}$
Barrier height between the saddle and the minimum	$0.5\varepsilon$

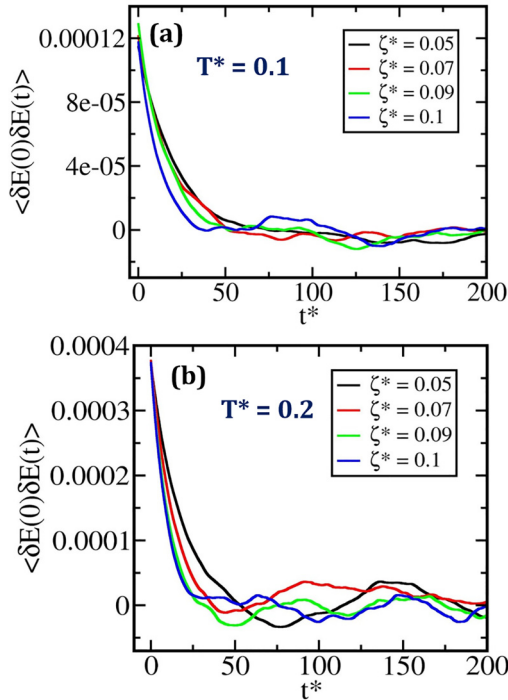


FIG. 8. Variations of the unnormalized energy relaxation function against time at two reduced temperatures (a)  $T^* = 0.1$  and (b)  $T^* = 0.2$ . It is observed that the relaxation of energy fluctuations  $\langle \delta E(0) \delta E(t) \rangle$  becomes faster with the increase in friction in both cases. Exponential fitting parameters are provided in Table I.

remains constant throughout the friction regime, as shown in Fig. 9.

Now, we turn to compute the escape rate directly from the simulation. There are several ways one can estimate the rate now from simulations.

(i) We can fit the population decay profile to a first-order exponential decay function. We shall refer to the rate obtained by this procedure as the phenomenological rate.

(ii) One of the important methods to get the escape rate is the mean first passage time (MFPT) formalism. In the MFPT (or first-order decay) formalism, we neglect the effects of the long-time correlated returns on the escape rate [57]. We, of course, include the immediate Kramers-type recrossing by placing the barrier away from the saddle. We discuss the variation of the escape rate obtained via the MFPT formalism against friction in more detail in SM-S7 [65].

(iii) To take into account the effect of long-range correlations, one can employ the method first introduced by Yamamoto and popularized by Chandler, and also used by Berne *et al.*, etc. [58].

We know that recrossing through the saddle reduces the escape rate. However, here the recrossing has a different origin in our context.

According to the Yamamoto-Chandler formalism, we introduce a correlation function to take into account the effects of recrossing, which is defined as [58–60]

$$C(t) = \frac{\langle h(0)h(t) \rangle}{\langle h(0) \rangle}. \quad (10)$$

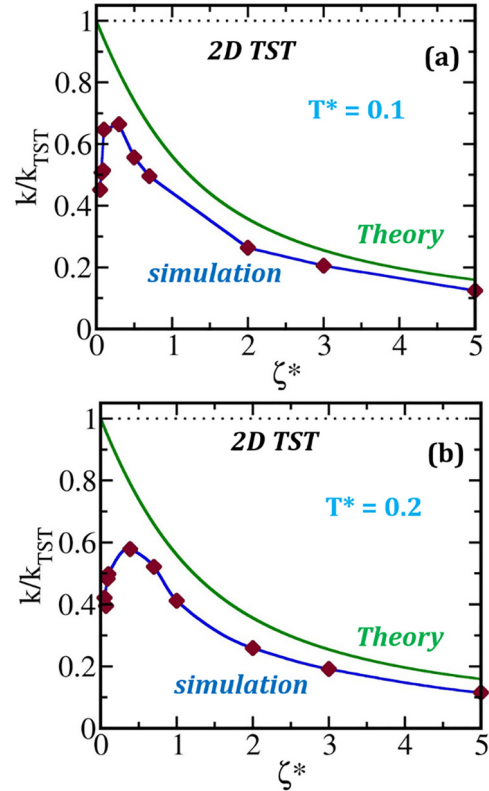


FIG. 9. Variation of the escape rate ( $k/k_{TST}$ ) against friction at two reduced temperatures (a)  $T^* = 0.1$  and (b)  $T^* = 0.2$ . Here  $k_{TST}$  denotes the two-dimensional transition state theory rate given by Eq. (12), and it is shown by the black dotted line. We use Langer's multidimensional rate theory to obtain the escape rate theoretically, as shown by the green line, to consider the effect of friction. The blue line connecting the brown data points indicates the variation of the rate obtained directly from simulation using the population decay formalism introduced by Yamamoto and Chandler. We have employed this formalism to consider the effect of long-time recrossing through the saddle. The line joining the data points is provided as a guide to the eyes.

Here  $h(t)$  is a Heaviside function, which is one when the particle is inside the original cell and becomes zero whenever the particle is outside the original cell. It is noted that  $h(0)$  always assumes the value of unity by this definition. For the rare transition between the two cells,  $C(t)$  approaches as  $C(t) \approx \langle h \rangle (1 - e^{-t/\tau_{rxn}})$ , where  $\tau_{rxn} = (k_1 + k_{-1})^{-1}$ . Here  $k_1$  and  $k_{-1}$  denote the forward and backward rates, respectively. If the reaction time  $\tau_{rxn}$  is much larger than the molecular time  $\tau_{mol}$ , there exists a time, i.e.,  $\tau_{mol} < t \ll \tau_{rxn}$ , in which  $C(t)$  grows linearly like  $C(t) \sim k_1 t$ . Consequently, reactive flux  $k(t) = \frac{dC(t)}{dt}$  exhibits a plateau region whose value determines the forward rate constant  $k_1$ . According to this definition, we calculate the forward rate constant and plot it against friction at two reduced temperatures, as shown by the brown points in Fig. 9. Simulation results show a nonmonotonic dependence of rate on friction, unlike theoretically predicted results.

In the limit of zero friction, the transition state theory or Kramer's theory fails for the following reasons [37,44,46]. When the friction is very low, the system fails to acquire the energy required to cross the barrier, as the sole energy

source via colliding with the surrounding solvent molecules decreases significantly in this limit. Therefore, unlike the high-friction limit, this limit has a proportional relation between friction and rate. Several attempts have been made to modify Kramer's theory to overcome the turnover issue in the low-friction limit [45,61]. In this regard, Skinner and Wolynes derived an expansion of rate in the powers of the friction coefficient, given by [62]

$$k = \frac{2\pi\zeta}{\omega_X^b} \left[ 1 + \frac{2\pi\zeta}{\omega_X^b} + \frac{(2\pi\zeta)^2}{2\pi} \right]^{-1} k_{\text{TST}}. \quad (11)$$

Here  $k_{\text{TST}}$  denotes the two-dimensional transition state theory rate constant, and it is given by [63]

$$k_{\text{TST}} = \left( \frac{\omega_Y^w}{\omega_Y^b} \right) \frac{\omega_X^w}{2\pi} \exp\left(-\frac{E^\ddagger}{k_B T}\right). \quad (12)$$

In Eq. (12),  $\omega_X^w$  is the well frequency along the reactive coordinate  $X$ ,  $\omega_Y^w$  is the frequency near the well along the orthogonal nonreactive coordinate  $Y$ , and  $\omega_Y^b$  denotes the harmonic frequency associated with the barrier along  $Y$ . In the overdamped limit, the multidimensional rate expression given by Eq. (9) reduces to the following equation:

$$k^{\text{SL}} = \left( \frac{\omega_X^b}{\zeta} \right) k_{\text{TST}}. \quad (13)$$

Equation (13) is popularly known as the Smoluchowski rate [9]. The regime where the diffusion or escape rate shows an inversely proportional relation with friction is known as the overdamped limit. From Fig. 9, it is clear that simulation results start converging with the theoretical predictions as we move to the overdamped regime. This is due to the reduction of the long-range correlated returns in the overdamped limit, discussed in the next section.

#### D. The random walk model estimates and comparisons

This section compares the diffusion obtained via a regular random walk model with the one directly obtained from simulation. According to the regular random walk model, diffusion ( $D$ ) is related to the rate constant ( $k$ ) via the relation [49]

$$D = \frac{1}{2d} k a^2.$$

Here,  $d$  denotes the dimension of the system, and  $a$  is the distance between the two adjacent minima. When the transitions between traps are uncorrelated, the random walk model can be used without approximation. However, these criteria are satisfied only when the particle spends sufficient time in each trapping region to forget its initial conditions. On the other hand, in the presence of correlation, the random walks traces the same path repeatedly by recrossing through the saddle point boundary. This makes the general expression  $D = (1/4) k a^2$  invalid. We shall come to this point in the next section.

On the other hand, we can directly calculate the escape rate ( $k$ ) of the particle from the simulation. We employ the formalism introduced by Yamamoto and Chandler to calculate the escape rate, considering the effects of correlated returns. We then extract the diffusion coefficient value by invoking the

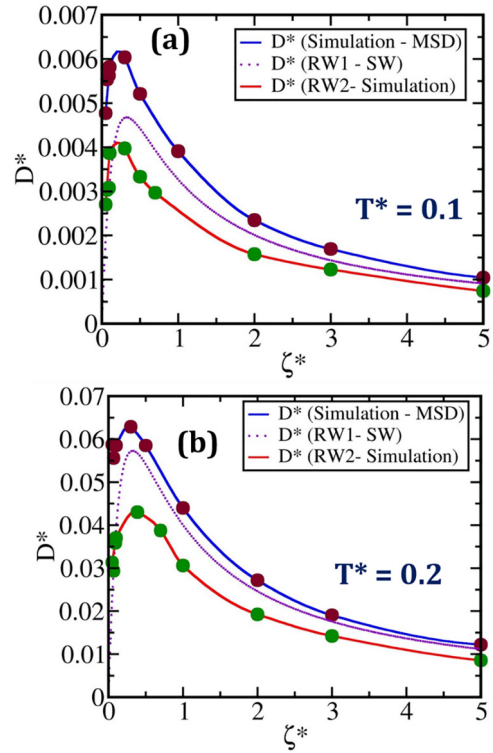


FIG. 10. The plot of the self-diffusion coefficient against friction at two reduced temperatures: (a)  $T^* = 0.1$  and (b)  $T^* = 0.2$ . The blue line connecting the brown data points represents the variation of the diffusion against friction obtained from the mean-square displacement (MSD) by the Langevin dynamics simulations. The line (blue trace) joining the data points is provided as a guide to the eyes. In theory, we employ the regular random walk model (RW), i.e.,  $D = 1/4 k a^2$ , to obtain the diffusion where the rate ( $k$ ) is extracted from different theoretical formalisms. The purple line (model RW1) shows the variation of diffusion against friction where  $k$  is predicted by Eq. (11)—the expression of Skinner and Wolynes. Similarly, we plot  $D$  obtained via the regular random walk model against friction, where  $k$  is calculated from simulation by employing the formalism introduced by Yamamoto and Chandler (model RW2, shown by the red line connecting the green data points). The line (red trace) joining the data points is provided as a guide to the eyes. From the plot, we observe that the random walk model predicts the diffusion well as we move to the overdamped limit. This is because, in the high-friction limit, noise destroys the correlated motion of the particle. But the theories fail in the intermediate-friction regime.

regular random walk model, as shown by the green circles in Fig. 10 (model RW2). We also obtain the diffusion using the regular random walk model, where Eq. (11), the rate theory of Skinner-Wolynes (SW), provides the escape rate [62]. The purple line represents the variation of this diffusion (model RW1) against friction. In Fig. 10, the blue line connecting the brown data points shows the variation of diffusion against friction obtained directly from simulation via MSD.

The plots presented in Fig. 10 show that the regular random walk model with rates obtained from both theory and simulation predicts the diffusion satisfactorily only in the high-friction regime. This is due to the fact that as we move into the high-friction regime, noise destroys the correlated

motion of the particle. As discussed before, the dissipation of excess energy becomes faster in the overdamped limit. Therefore, the diffusion predicted by both random walk models (RW1 and RW2) shows acceptable convergence to the actual diffusion in this regime.

### E. Modification of the random walk model in the presence of correlated returns

The disagreement between theoretical and simulation results, particularly in the low-friction regime, as shown in Fig. 10, proposes a modification in the theory of the regular random walk model employed here. To address the effect of correlated returns, we follow the formalism introduced by Hynes [64]. According to the formalism, the transition state theory rate constant can be modified in the presence of correlated random walks as

$$k(T) = \langle J_e(S) \rangle_e + \int_0^{T_M} dt \langle J_e(S) J_R(S, t) \rangle_e, \quad (14)$$

where  $J_e(S)$  and  $J_R(S, t)$  are the outgoing flux crossing the saddle surface  $S$  at time  $t = 0$  and intrinsically negative flux coming back to the initial surface at later  $t$ . The second term is mainly responsible for lowering the value of the rate constant. In Eq. (14), the subscript “ $e$ ” denotes the equilibrium average in the canonical ensemble, and  $T_M$  is the upper limit of integration to neglect the contribution coming from the long-time “thermalized” returns. We can further modify Eq. (14) as

$$k(T) = \langle J(S) \rangle \left[ 1 - \int_0^{T_M} P_R(t) dt \right]. \quad (15)$$

Here  $P_R(t)$  is the conditional probability of return at time  $t$  to the initial cell, provided the particle crossed the saddle boundary at  $t = 0$  to enter the neighbor cells.  $\langle J(S) \rangle$  is the rate constant without the effects of long-term correlated returns. We define a term as  $f(T_M) = \int_0^{T_M} P_R(t) dt$ , which measures the fraction of returns within the cutoff time  $T_M$ . We show the variation of  $f(T_M)$  against the cutoff time  $T_M$  for different friction values in Fig. S8 of the SM [65]. The plot demonstrates that a well-defined plateau region follows a sharp rise in all the cases. The sharp rise is due to the oscillatory nature of the returning trajectories with a well-defined frequency. The value of  $f(T_M)$  at the plateau region is plotted against friction in Fig. 11(a) at a reduced temperature  $T^* = 0.1$ . The existence of the plateau region is due to the separation of timescales between correlated returns and thermalized returns. In Fig. 11(a), the probability of correlated returns increases with increasing friction in the high-friction regime. However, in the low to intermediate damping region, initially, it shows a slight decrease followed by a sharp rise after passing through a minimum. In Fig. 11(b), we plot the rate constant against friction employing Eq. (15) at  $T^* = 0.1$ , and we find that the predicted rate constant deviates slightly from the actual values in the low-friction regime. It is important to note that we consider only a single recrossing to obtain the rate. However, the trajectory analysis confirms that the system suffers multiple recrossing at the saddle. Therefore, multiple recrossings need to be considered to address the appearance of a slight deviation in the low-damping region.

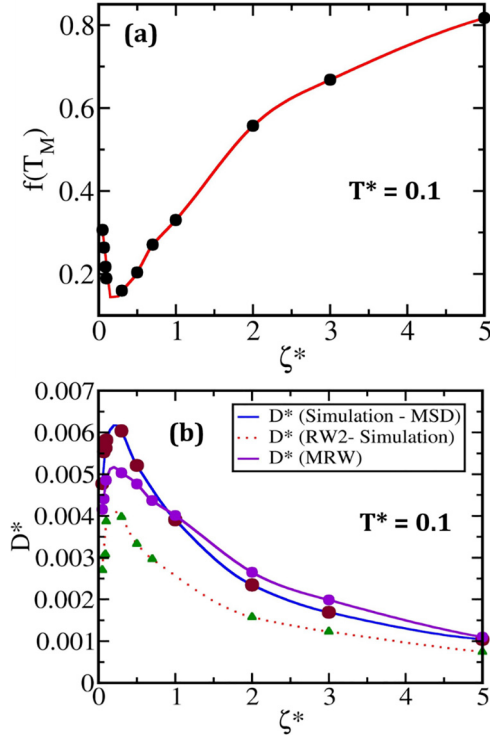


FIG. 11. (a) The plot of the return probability against friction (in the range 0.05–5.0) at a reduced temperature  $T^* = 0.1$ . We find that the probability of correlated returns increases with the increase in friction in the high-friction regime. However, in the low to intermediate damping region, initially, it shows a slight decrease followed by a sharp rise after passing through a minimum. (b) The plot of the diffusion coefficient against friction. The purple line connecting the data points shows the variation of diffusion against friction where  $k$  is predicted by Eq. (15)—the expression of the modified random walk model (MRW). For comparison, the result predicted by the regular random walk model with  $k$  obtained from simulation (i.e., using the formalism introduced by Yamamoto and Chandler) is also shown by the red dotted line as a reference. The blue line connecting the data points indicates the variation of diffusion directly obtained from simulation via MSD, as discussed earlier. Here lines joining the data points are provided as a guide to the eyes.

### F. Entropy and diffusion

There have been considerable discussions on the relationship between diffusion and entropy. Entropy is a measure of the configuration space available to the system, while diffusion is the rate of exploration of this configuration. In the liquid regime, this relation is straightforward, as discussed before. However, when diffusion occurs on a multidimensional energy landscape where the solute or the system has to cross barriers, the relation between diffusion and entropy becomes nontrivial.

On the other hand, according to the celebrated transition state theory of Wigner and Eyring, the rate constant is a property of phase space dynamics [44,63,66]. We use this connection to relate diffusion with entropy. In a recent article, we presented a microscopic derivation of the exponential relation between diffusion and entropy starting from the basic principles of statistical mechanics in both canonical

and microcanonical ensembles [67]. This section presents a derivation of an exponential scaling relation between diffusion and entropy in a system where a massive Brownian particle is coupled with a heat bath at temperature  $T$ . Therefore, the solute particle follows an ordinary Langevin equation defined by Eq. (5) with a coupling constant  $\zeta$ . In a canonical ensemble, rate constant  $k(T)$  is given by [67–69]

$$k(T) = \frac{\frac{1}{2} \frac{1}{(2\pi\hbar)^{Nd}} \int \int dq^N dp^N \exp(-\beta H_N) \delta(q_1 - q^\dagger) |\dot{q}_1|}{\frac{1}{(2\pi\hbar)^{Nd}} \int \int dq^N dp^N \exp(-\beta H_N)}. \quad (16)$$

In Eq. (16),  $H_N$  denotes the total Hamiltonian of the system with  $N$  degrees of freedom and is given by  $H_N = \sum_{i=1}^{Nd} \frac{p_i^2}{2M} + V_N(q_1, q_2, \dots, q_N)$ . Here  $q^\dagger$  is the location of the saddle along the reaction coordinate  $q_1$ , and  $M$  is the mass of the Brownian particle. Before proceeding further, we assume that the potential of the Brownian particle takes the form near the saddle [70]

$$V_N = E(0) + \sum_{i=1}^N \frac{M}{2} \zeta^2 (q_i - q^\dagger)^2, \quad (17)$$

where  $E(0)$  is the potential energy at the saddle point without noise. We then simplify the denominator of Eq. (16) (i.e., denoted by  $Q$ ) to obtain

$$Q = \left( \frac{k_B T}{\hbar \zeta} \right)^{Nd} \exp\left(-\frac{E(0)}{k_B T}\right). \quad (18)$$

In a canonical ensemble, entropy is related to the partition function ( $Q$ ) through a relation like  $S = k_B \frac{\partial}{\partial T} (T \ln Q)$ . We then employ the relation between entropy and partition function to rewrite  $Q$  in terms of  $S$  as

$$Q = \exp\left(\frac{S}{k_B}\right) \exp\left(-Nd - \frac{E(0)}{k_B T}\right). \quad (19)$$

In a similar way, we simplify the numerator of Eq. (16) to obtain

$$\frac{k_B T}{2\pi\hbar} \exp\left(\frac{S^\dagger}{k_B}\right) \exp\left(-(N-1)d - \frac{E(0)}{k_B T}\right). \quad (20)$$

We define  $Q^\dagger$  as the partition function of the system at the saddle point without the reactive motion. Effectively  $Q^\dagger$  possesses one less vibrational degree of freedom compared to the canonical partition function  $Q$  for the reactant state. With the same analogy, we can establish the following relation between the configurational entropy and partition function at the saddle point as  $S^\dagger = k_B \frac{\partial}{\partial T} (T \ln Q^\dagger)$ . Here  $S^\dagger$  is the configurational entropy without the reactive mode [67].

By taking the ratio of Eqs. (19) and (20), we obtain the following expression for the rate constant, given by

$$k(T) = \left( \frac{k_B T}{h} \right) e^d \exp\left(-\frac{(S - S^\dagger)}{k_B}\right). \quad (21)$$

We then invoke the random walk formalism, i.e.,  $D = \frac{1}{2d} ka^2$ , where  $d$  denotes the dimension of the system, described earlier to obtain the following expression for the

diffusion:

$$D = \frac{a^2}{2d} \left( \frac{k_B T}{h} \right) e^d \exp\left(-\frac{(S - S^\dagger)}{k_B}\right). \quad (22)$$

It is similar to the form of Rosenfeld but not identical [67,71]. According to the Rosenfeld scaling relation, diffusion is related to entropy ( $S$ ) via the relation  $D^* = a \exp(b \frac{S - S_{id}}{Nk_B})$ . Here  $D^*$  is the reduced self-diffusion coefficient,  $S_{id}$  is the total entropy of the ideal gas,  $a$  and  $b$  are two scaling constants, and  $N$  denotes the total number of atoms/molecules present in the system. In Eq. (22),  $S^\dagger$  is a scaling constant that serves the same role as  $S_{id}$  involved in the Rosenfeld scaling relation. We can compute  $S^\dagger$  by exponentially fitting the plot of diffusion against entropy with the aid of Eq. (22).

We hope to explore the relationship between diffusion and entropy by computing the configurational entropy for this system in the future.

#### IV. CONCLUSION

The study of diffusion in a multidimensional energy surface has been a subject of immense interest in many branches of physics, chemistry, and biology to discuss diverse problems. To interrogate the role of noise in such diffusion processes, we study the diffusional dynamics of a Brownian particle in a periodic and continuous-potential analog of regular Lorentz gas. The system of interest can also be relevant to a variety of applications, such as superionic conductors, the motion of adsorbates on crystal surfaces, polymers diffusing at the interfaces, molecular graphene, etc. We observe a nonmonotonic dependence of diffusion as a function of friction in this two-dimensional periodic system. We explain the nonmonotonic dependence of diffusion by invoking the random walk model with the rate given by an appropriate two-dimensional rate theory. The presence of coherence in the trajectory in the low-friction limit gives rise to an exciting complexity that can be understood by using the Lyapunov exponent.

It is not clear *a priori* that a random walk model based analytical theory with an accurate rate calculation can reproduce the nonmonotonic friction dependence of the diffusion constant. In fact, the Padé approximant in the theory of Skinner-Wolynes is reasonably satisfactory in describing this nonmonotonic dependence.

Although diffusion in the absence of noise is in itself a fascinating feature for this Hamiltonian system and has not really been studied in detail, our emphasis here is on the combined role of noise and energy landscape on diffusive motions. In the absence of noise, the particle gets trapped at the minimum of the initial cell and exhibits a pronounced oscillatory behavior in the plot of velocity autocorrelation against time. However, noise destroys the coherence by randomizing the motion of the particle. This study demonstrates how the combined effect of noise and the curvature of the potential energy landscape plays an essential role in inducing oscillations in the plot of a velocity correlation function against time.

Trajectory analysis confirms that the particle suffers multiple long-range returns by crossing and recrossing the saddle in the low-friction limit. Such long-range crossing and recrossing through the saddle are different from those usu-

ally discussed in the context of barrier crossing dynamics, especially in relation to the theories of Kramers and Smoluchowski. The ones we focus on return from other cells after rebounding from the maxima in other cells. These are not due to noise-generated solvent collisions.

In the presence of such correlated returns, the onset of chaotic motion is an interesting problem that needs to be studied. As we remarked earlier, the concave nature of the surface potential induces refocusing of the trajectories that leave one cell and enter the next adjoining cell. To characterize the motion of the particle quantitatively, we calculate the Lyapunov exponent for this system and plot it against friction. We observe a nearly saturated region following a sharp rise in  $L_n$  against friction in each case (i.e.,  $T^* = 0.1$  and  $0.2$ ), and we address this issue in detail. Our study demonstrates that both noise and the potential energy landscape play a vital role in influencing the divergence rate of two close trajectories in configurational space.

Although we have used a two-dimensional periodic landscape, the results are expected to remain valid in three and higher dimensions. Such a generalization was observed earlier for diffusion on rugged energy landscapes [72].

To validate the random walk model in such a complex dynamical system in the presence of the long-range return of trajectories, we require the rate of escape from one cell to an adjacent cell. At the same time, in a recent study, we attempted to analyze the rate of barrier crossing dynamics in a more complex two-dimensional reaction energy surface for insulin dimer dissociation [27]. In that case, a quantitatively accurate estimate of the rate required to validate the theoretical predictions was not available. Due to the simplicity of this deterministic model system, we can not only predict the rate by various theoretical approaches, but we also obtain a quantitatively accurate rate directly from simulations without making approximations.

We theoretically employ the multidimensional rate theory, like the two-dimensional transition state theory and Langer's theory, to compute the escape rate. To obtain the escape rate directly from simulation, we invoke the mean first passage time formalism and the scheme developed by Yamamoto and Chandler, considering the effect of long-term recrossing. We

find that Langer's theory can explain the high-friction region semiquantitatively but not the low-friction domain. Thus, it fails to provide a nonmonotonic friction dependence.

We next model the diffusion as a random walk in a two-dimensional lattice and invoke the relation between diffusion and rate (i.e.,  $D = 1/4ka^2$ ) to calculate the diffusion with  $k$  obtained from the simulation. We compare that diffusion with the diffusion directly obtained via MSD to validate the random walk model. With the increasing strength of the noise, the random walk model starts to predict a more accurate value for the diffusion since noise destroys the existing long-term correlated motions. Our study clearly shows that the long-term correlated returns induced by the concave region of the surface play a significant role in lowering diffusion. To understand the deviation in the low-friction regime, we adopt a theoretical formalism following the approach introduced by Hynes. We explicitly estimate the return probability for the initial cell for different friction values, and we calculate the escape rate. As is evident in our study, the modified random walk model provides better results than the regular random walk model, specifically in the low-friction regime. The appearance of a slight deviation is due to the consideration of single recrossing, which suggests multiple recrossing needs to be considered in the low-friction regime to obtain a more accurate value.

The relationship between diffusion and entropy is highly intriguing since it relates to two seemingly different properties: structure and dynamics. In this context, we present a microscopic derivation of the exponential relationship between diffusion and entropy for a system coupled with a heat bath at a particular temperature starting from the basic principles of statistical mechanics. We hope to explore the derived relation between diffusion and entropy in our system in the near future.

## ACKNOWLEDGMENTS

B.B. thanks SERB (DST), India, for a National Science Chair (NSC) Professorship, and SERB (DST), India, for partial funding of this work. S.A. thanks IISc for the research fellowship.

- 
- [1] A. Einstein, Investigations on the theory of the brownian movement, *Ann. Phys.* **17**, 549 (1905).
  - [2] R. Zwanzig, *Nonequilibrium Statistical Mechanics* (Oxford University Press, Oxford, 2001).
  - [3] B. Bagchi, *Molecular Relaxation in Liquids* (Oxford University Press, New York, 2012).
  - [4] J. N. Onuchic, Z. Luthey-Schulten, and P. G. Wolynes, Theory of protein folding: The energy landscape perspective, *Annu. Rev. Phys. Chem.* **48**, 545 (1997).
  - [5] J. D. Bryngelson and P. G. Wolynes, Intermediates and barrier crossing in a random energy model (with applications to protein folding), *J. Phys. Chem.* **93**, 6902 (1989).
  - [6] J. D. Bryngelson and P. G. Wolynes, Spin glasses and the statistical mechanics of protein folding, *Proc. Natl. Acad. Sci. (U.S.A.)* **84**, 7524 (1987).
  - [7] M. Di Pierro, D. A. Potoyan, P. G. Wolynes, and J. N. Onuchic, Anomalous diffusion, spatial coherence, and viscoelasticity from the energy landscape of human chromosomes, *Proc. Natl. Acad. Sci. (U.S.A.)* **115**, 7753 (2018).
  - [8] N. D. Socci, J. N. Onuchic, and P. G. Wolynes, Diffusive dynamics of the reaction coordinate for protein folding funnels, *J. Chem. Phys.* **104**, 5860 (1996).
  - [9] M. Smoluchowski, On the kinetic theory of the brownian molecular motion and of suspensions, *Ann. Phys.* **21**, 756 (1906).
  - [10] R. R. Netz and W. A. Eaton, Estimating computational limits on theoretical descriptions of biological cells, *Proc. Natl. Acad. Sci. (U.S.A.)* **118**, 1 (2021).
  - [11] R. Zwanzig, Diffusion in a rough potential, *Proc. Natl. Acad. Sci. (U.S.A.)* **85**, 2029 (1988).

- [12] T. H. Gray and E. H. Yong, Effective diffusion in one-dimensional rough potential-energy landscape, *Phys. Rev. E* **102**, 022138 (2020).
- [13] D. L. Stein and C. M. Newman, Broken ergodicity and the geometry of rugged landscapes, *Phys. Rev. E* **51**, 5228 (1995).
- [14] S. Banerjee, R. Biswas, K. Seki, and B. Bagchi, Diffusion on a rugged energy landscape with spatial correlations, *J. Chem. Phys.* **141**, 124105 (2014).
- [15] K. Seki and B. Bagchi, Relationship between entropy and diffusion: A statistical mechanical derivation of rosenfeld expression for a rugged energy landscape, *J. Chem. Phys.* **143**, 194110 (2015).
- [16] R. Festa and E. G. d'Agliano, Diffusion coefficient for a brownian particle in a periodic field of force, *Physica A* **90**, 229 (1978).
- [17] J. S. Langer, Statistical theory of the decay of metastable states, *Ann. Phys. (N.Y.)* **54**, 258 (1969).
- [18] P. Bhimalapuram, S. Chakrabarty, and B. Bagchi, Elucidating the Mechanism of Nucleation near the Gas-Liquid Spinodal, *Phys. Rev. Lett.* **98**, 206104 (2007).
- [19] R. Ghosh, S. Roy, and B. Bagchi, Multidimensional free energy surface of unfolding of HP-36: Microscopic origin of ruggedness, *J. Chem. Phys.* **141**, 135101 (2014)..
- [20] E. Hershkovitz, P. Talkner, E. Pollak, and Y. Georgievskii, Multiple hops in multidimensional activated surface diffusion, *Surf. Sci.* **421**, 73 (1999).
- [21] S. Acharya and B. Bagchi, Non-markovian rate theory on a multidimensional reaction surface: Complex interplay between enhanced configuration space and memory, *J. Chem. Phys.* **156**, 134101 (2022).
- [22] A. Ma, A. Nag, and A. R. Dinner, Dynamic coupling between coordinates in a model for biomolecular isomerization, *J. Chem. Phys.* **124**, 144911 (2006).
- [23] C. Ayaz, L. Tepper, F. N. Brünig, J. Kappler, J. O. Daldrop, and R. R. Netz, Non-markovian modeling of protein folding, *Proc. Natl. Acad. Sci. (U.S.A.)* **118**, 20 (2021).
- [24] J. F. Dama, G. Rotskoff, M. Parrinello, and G. A. Voth, Transition-tempered metadynamics: Robust, convergent metadynamics via on-the-fly transition barrier estimation, *J. Chem. Theor. Comput.* **10**, 3626 (2014).
- [25] S. Paul and S. Taraphder, Determination of the reaction coordinate for a key conformational fluctuation in human carbonic anhydrase II, *J. Phys. Chem. B* **119**, 11403 (2015).
- [26] S. Paul, T. K. Paul, and S. Taraphder, Reaction coordinate, free energy, and rate of intramolecular proton transfer in human carbonic anhydrase II, *J. Phys. Chem. B* **122**, 2851 (2018).
- [27] S. Acharya, S. Mondal, S. Mukherjee, and B. Bagchi, Rate of insulin dimer dissociation: Interplay between memory effects and higher dimensionality, *J. Phys. Chem. B* **125**, 9678 (2021).
- [28] S. Mukherjee, S. Acharya, S. Mondal, P. Banerjee, and B. Bagchi, Structural stability of insulin oligomers and protein association-dissociation processes: Free energy landscape and universal role of water, *J. Phys. Chem. B* **125**, 11793 (2021).
- [29] J. S. Langer, Theory of the condensation point, *Ann. Phys. (N.Y.)* **41**, 108 (1967).
- [30] P. Hanggi, P. Talkner, and M. Borkovec, Reaction-rate theory: Fifty years after kramers, *Rev. Mod. Phys.* **62**, 251 (1990).
- [31] B. Bagchi, Fractional viscosity dependence of relaxation rates and non-steady-state dynamics in barrierless reactions in solution, *Chem. Phys. Lett.* **138**, 315 (1987).
- [32] B. Bagchi, R. Zwanzig, and M. C. Marchetti, Diffusion in a two-dimensional periodic potential, *Phys. Rev. A* **31**, 892 (1985).
- [33] V. V. Ignatyuk, A temperature behavior of the frustrated translational mode of adsorbate and the nature of the "adsorbate-substrate, *J. Chem. Phys.* **136**, 184104 (2012).
- [34] K. J. Challis and M. W. Jack, Tight-binding approach to overdamped brownian motion on a multidimensional tilted periodic potential, *Phys. Rev. E* **87**, 052102 (2013).
- [35] M. Gibertini, A. Singha, V. Pellegrini, M. Polini, G. Vignale, A. Pinczuk, L. N. Pfeiffer, and K. W. West, Engineering artificial graphene in a two-dimensional electron gas, *Phys. Rev. B* **79**, 241406(R) (2009).
- [36] D. L. Ermak and H. Buckholz, Numerical integration of the langevin equation: Monte carlo simulation, *J. Comput. Phys.* **35**, 169 (1980).
- [37] J. D. Bao, R. W. Li, and W. Wu, Numerical simulations of generalized langevin equations with deeply asymptotic parameters, *J. Comput. Phys.* **197**, 241 (2004).
- [38] M. P. Allen and D. J. Tildesley, *Computer Simulation of Liquids* (Oxford University Press, New York, 1989).
- [39] G. G. Putzel, M. Tagliazucchi, and I. Szleifer, Nonmonotonic Diffusion of Particles among Larger Attractive Crowding Spheres, *Phys. Rev. Lett.* **113**, 138302 (2014).
- [40] S. H. Courtney, G. R. Fleming, L. R. Khundkar, and A. H. Zewail, Unimolecular reaction rates in solution and in the isolated molecule: Comparison of diphenyl butadiene nonradiative decay in solutions and supersonic jets, *J. Chem. Phys.* **80**, 4559 (1984).
- [41] L. A. Bunimovich and Y. G. Sinai, Markov partitions for dispersed billiards, *Commun. Math. Phys.* **78**, 247 (1980).
- [42] J. Machta and R. Zwanzig, Diffusion in a Periodic Lorentz Gas, *Phys. Rev. Lett.* **50**, 1959 (1983).
- [43] S. Acharya and B. Bagchi, Study of entropy-diffusion relation in deterministic hamiltonian systems through microscopic analysis, *J. Chem. Phys.* **153**, 184701 (2020).
- [44] J. P. Eckmann and D. Ruelle, Ergodic theory of chaos and strange attractors, *Rev. Mod. Phys.* **57**, 617 (1985).
- [45] G. D. Charó, M. D. Chekroun, D. Sciamarella, and M. Ghil, Noise-driven topological changes in chaotic dynamics, *Chaos* **31**, 103115 (2021).
- [46] P. Gaspard and G. Nocolis, Transport Properties, Lyapunov Exponents, and Entropy Per Unit Time, *Phys. Rev. Lett.* **65**, 1693 (1990).
- [47] T. Hofmann and J. Merker, On local lyapunov exponents of chaotic hamiltonian systems, *CMST* **24**, 97 (2018).
- [48] I. I. Shevchenko and A. V. Melnikov, Lyapunov exponents in the hénon-heiles problem, *JETP Lett.* **77**, 642 (2003).
- [49] S. Chandrasekhar, Stochastic problems in physics and astronomy, *Rev. Mod. Phys.* **15**, 1 (1943).
- [50] H. Eyring, The activated complex in chemical reactions, *J. Chem. Phys.* **3**, 107 (1935).
- [51] H. Grabert, Escape from a Metastable Well: The Kramers Turnover Problem, *Phys. Rev. Lett.* **61**, 1683 (1988).
- [52] H. A. Kramers, Brownian motion in a field of force and the diffusion model of chemical reactions, *Physica* **7**, 284 (1940).
- [53] R. Landauer and J. A. Swanson, Frequency factors in the thermally activated process, *Phys. Rev.* **121**, 1668 (1961).

- [54] G. Van Der Zwan and J. T. Hynes, Reactive paths in the diffusion limit, *J. Chem. Phys.* **77**, 1295 (1982).
- [55] D. G. Truhlar and B. C. Garrett, Multidimensional transition state theory and the validity of grote-hynes theory, *J. Phys. Chem. B* **104**, 1069 (2000).
- [56] A. Debnath, R. Chakrabarti, and K. L. Sebastian, Rate processes with dynamical disorder: A direct variational approach, *J. Chem. Phys.* **124**, 204111 (2006).
- [57] R. Müller, P. Talkner, and P. Reimann, Rates and mean first passage times, *Phys. A Stat. Mech. Appl.* **247**, 338 (1997).
- [58] J. A. Montgomery, D. Chandler, and B. J. Berne, Trajectory analysis of a kinetic theory for isomerization dynamics in condensed phases, *J. Chem. Phys.* **70**, 4056 (1979).
- [59] C. Dellago, P. G. Bolhuis, F. S. Csajka, and D. Chandler, Transition path sampling and the calculation of rate constants, *J. Chem. Phys.* **108**, 1964 (1998).
- [60] C. Dellago, P. G. Bolhuis, and D. Chandler, On the calculation of reaction rate constants in the transition path ensemble, *J. Chem. Phys.* **110**, 6617 (1999).
- [61] M. Lee, G. R. Holtom, and R. M. Hochstrasser, Observation of the Kramers turnover region in the isomerism of trans-stilbene in fluid ethane, *Chem. Phys. Lett.* **118**, 359 (1985).
- [62] J. L. Skinner and P. G. Wolynes, Relaxation processes and chemical kinetics, *J. Chem. Phys.* **69**, 2143 (1978).
- [63] P. Pechukas, Transition state theory, *Annu. Rev. Phys. Chem.* **32**, 159 (1981).
- [64] S. H. Northrup and J. T. Hynes, The stable states picture of chemical reactions. I. Formulation for rate constants and initial condition effects, *J. Chem. Phys.* **73**, 2700 (1980).
- [65] See Supplemental Material at <http://link.aps.org/supplemental/10.1103/PhysRevE.107.024127> for power spectrum of velocity correlation function, MSD against time, Renormalization procedure, Lyapunov exponent against time, Role of noise and variation of total energy against time, Energy correlation function and power spectrum, Calculation of rate using mean first passage time formalism, and Return Probability against cut-off time.
- [66] K. J. Laidler, *Chemical Kinetics* (McGraw Hill, New York, 1965).
- [67] A. Lohle and J. Kastner, Calculation of reaction rate constants in the canonical and microcanonical ensemble, *J. Chem. Theor. Comput.* **14**, 5489 (2018).
- [68] J. D. Doll, A unified theory of dissociation, *J. Chem. Phys.* **73**, 2760 (1980).
- [69] H. W. Schranz, L. M. Raff, and D. L. Thompson, Correspondence of canonical and microcanonical rate constants using variational transition state theory for simple bond fissions, *Chem. Phys. Lett.* **171**, 68 (1990).
- [70] Y. Liao and X.-B. Gong, A new derivation of the relationship between diffusion coefficient and entropy in classical brownian motion by the ensemble method, *SciPost Phys. Core* **4**, 1 (2021).
- [71] Y. Rosenfeld, Relation between the transport coefficient and the internal entropy of simple systems, *Phys. Rev. A* **15**, 2545 (1977).
- [72] K. Seki, K. Bagchi, and B. Bagchi, Anomalous dimensionality dependence of diffusion in a rugged energy landscape: How pathological is one dimension?, *J. Chem. Phys.* **144**, 194106 (2016).